JACS
JOURNAL OF THE AMERICAN CHEMICAL SOCIETY

ARTICLE

pubs.acs.org/JACS

Mechanistic Investigation and Reaction Kinetics of the Low-Pressure Copolymerization of Cyclohexene Oxide and Carbon Dioxide Catalyzed by a Dizinc Complex

Fabian Jutz,[†] Antoine Buchard,[†] Michael R. Kember,[†] Siw Bodil Fredriksen,[‡] and Charlotte K. Williams*[,†]

[†]Department of Chemistry, Imperial College London, London SW7 2AZ, UK

[‡]Norner AS, Asdalstrand 291, 3960 Stathelle, Norway

Supporting Information

ABSTRACT: The reaction kinetics of the copolymerization of carbon dioxide and cyclohexene oxide to produce poly(cyclohexene carbonate), catalyzed by a dizinc acetate complex, is studied by in situ attenuated total reflectance infrared (ATR-IR) and proton nuclear magnetic resonance (^{1}H NMR) spectroscopy. A parameter study, including reactant and catalyst concentration and carbon dioxide pressure, reveals zero reaction order in carbon dioxide concentration, for pressures between 1 and 40 bar and temperatures up to 80 °C, and a first-order dependence on catalyst concentration and concentration of cyclohexene oxide. The activation energies for the formation of poly(cyclohexene carbonate) and the cyclic side product cyclohexene carbonate are calculated, by determining the rate coefficients over a temperature range between 65 and 90 °C and using Arrhenius plots, to be 96.8 ± 1.6 kJ mol^{-1} (23.1 kcal mol^{-1}) and 137.5 ± 6.4 kJ mol^{-1} (32.9 kcal mol^{-1}), respectively. Gel permeation chromatography (GPC), ^{1}H NMR spectroscopy, and matrix-assisted laser desorption/ionization time-of-flight (MALDI-ToF) mass spectrometry are employed to study the poly(cyclohexene carbonate) produced, and reveal bimodal molecular weight distributions, with narrow polydispersity indices (≤1.2). In all cases, two molecular weight distributions are observed, the higher value being approximately double the molecular weight of the lower value; this finding is seemingly independent of copolymerization conversion or reaction parameters. The copolymer characterization data and additional experiments in which chain transfer agents are added to copolymerization experiments indicate that rapid chain transfer reactions occur and allow an explanation for the observed bimodal molecular weight distributions. The spectroscopic and kinetic analyses enable a mechanism to be proposed for both the copolymerization reaction and possible side reactions; a dinuclear copolymerization active site is implicated.

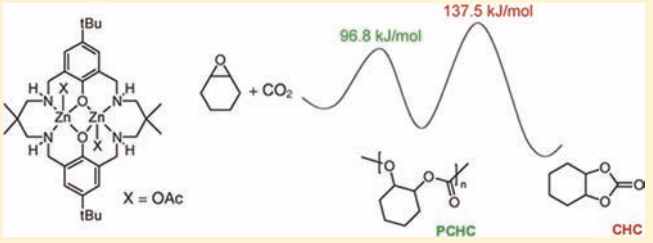

INTRODUCTION

Environmental and economical concerns associated with depleting oil resources have triggered a growing interest in the chemical conversion of carbon dioxide (CO_2), so as to enable its use as a renewable carbon source. CO_2 is, despite its low reactivity, a highly attractive carbon feedstock, as it is inexpensive, virtually nontoxic, abundantly available in high purity, and nonhazardous. Therefore, CO_2 could be a promising substitute for substances such as carbon monoxide or phosgene in many processes.[1] One of the developing applications of CO_2 is the copolymerization with epoxides to yield aliphatic polycarbonates, a field pioneered by Inoue et al. more than 40 years ago.[2] Several metal-based catalytic systems for this reaction have been reported, including the use of either homogeneous or heterogeneous catalysts. An overview on the present state of this research can be found in several comprehensive reviews.[3] Among the epoxides employed in the copolymerization, cyclohexene oxide (CHO) has received special interest,[3c,4] as the product, poly(cyclohexene carbonate) (PCHC), shows a high glass transition temperature and reasonable tensile strength, while being conveniently degradable.[5] As CO_2 is the thermodynamic sink of carbon, its chemical activation requires highly efficient catalysts and often necessitates processes operating at elevated temperatures and pressures. Among the most active homogeneous copolymerization catalysts are zinc β-diiminate complexes[4c,6] and chromium(III) or cobalt(III) salen complexes,[3c,4a,7] both of which require several bar of CO_2. In an elegant study, Coates and co-workers established that the most active zinc β-diiminate complexes were, in fact, dimers under the conditions of the catalysis.[4c] Kinetic studies using metal salen catalysts depend on the presence/absence of cocatalysts;[8] however, very recently the groups of Rieger and Nozaki have deliberately targeted dinuclear salen catalysts, which are highly effective.[9] One rationale is that a so-called bimetallic (dinuclear) mechanism occurs that requires two metal centers for the epoxide coordination and subsequent insertion chemistries.[3b,9] This hypothesis has triggered the development of ancillary

Received: July 11, 2011
Published: October 05, 2011

Scheme 1. Structure of Complex 1 and the Reaction between CO_2 and CHO Producing Poly(cyclohexene) Carbonate (PCHC) and a Byproduct, Cyclohexene Carbonate (CHC)

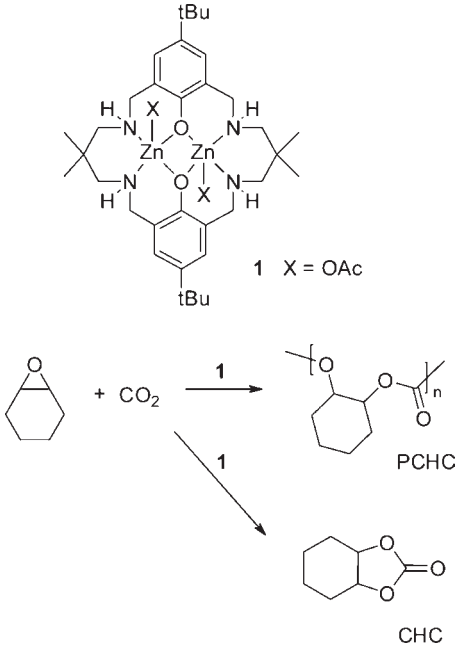

ligands and catalysts deliberately designed to bind two metal centers in close proximity, and some of the dizinc catalysts have proved to be especially effective.[3f,10] Our group recently reported an air-stable dizinc acetate complex, coordinated by a macrocyclic ligand, **1** (Scheme 1), which shows high catalytic activity, even at ambient CO_2 pressure.[11] The catalyst exhibits excellent copolymerization selectivity, giving high proportions of carbonate repeat units and low yields of cyclic cyclohexene carbonate (CHC) byproduct. The same macrocyclic ligand was also used with other metal centers [Co(II/III),[12] Fe(III)[13]], which proved to be excellent catalysts as well. Complex **1** is a rare example of a catalyst that is capable of high activity at ambient pressure (1 bar) of CO_2,[14] yielding PCHC of moderate molecular weight, with narrow polydispersity index (PDI), and reaches remarkably high turnover numbers (TON). The high activity of this catalyst also motivated a very recently published computational study by Rieger and co-workers, focusing on the lack of polymerization using propylene oxide and CO_2.[15] Any further improvements to the catalyst and an understanding of its properties are dependent on understanding the copolymerization mechanism on a molecular level. Such mechanistic insight is also likely to be relevant to other catalysts for the activation and copolymerisation of CO_2. Herein, we report the use of complementary spectroscopic techniques for a detailed reaction parameter study of the copolymerization kinetics using **1**, an analysis of the activation energies for PCHC and CHC, and a proposed dinuclear mechanism to account for the experimental findings. This study also addresses the molecular weight distributions of the resulting PCHC and proposes a mechanism invoking chain transfer with diol and hydroxyl moieties, to account for the bimodal molecular weight distributions of the resulting PCHC.

EXPERIMENTAL SECTION

Reagents and Methods. The catalyst $[LZn_2(OAc)_2]$ (**1**) was synthesized by employing the previously published method.[11] All solvents and reagents were purchased from commercial sources (Sigma-Aldrich, Strem Chemicals, and Alfa Aesar). Cyclohexene oxide was fractionally distilled over calcium hydride prior to use and stored under a nitrogen atmosphere. Research grade CO_2 for copolymerization reactions was purchased from BOC (Linde Gas). Anhydrous diethyl carbonate (DEC) was purchased from Aldrich and used without further purification.

^{1}H NMR spectra were measured in $CDCl_3$ on a Bruker AV-400 spectrometer. MALDI-ToF spectrometry measurements were performed using a Fisons Analytical (VG) Autospec spectrometer. The samples were dissolved in THF together with the dithranol matrix and the cationizing additive potassium trifluoroacetate in a ratio 10:10:1. In situ ATR-FTIR measurements were performed on a Mettler-Toledo ReactIR 4000 spectrometer equipped with a MCT detector and a silver halide DiComp probe. Gel permeation chromatography (GPC) data were collected using a Polymer Laboratories PL GPC-50 instrument with THF as the eluent, at a flow rate of 1 mL min^{-1} and narrow M_w polystyrene standards for calibration.

Copolymerization Procedures. Reactions using 1 bar of CO_2 were performed in a Schlenk tube connected to a manifold line (vacuum/CO_2) and heated using an oil bath. In a typical experiment, a defined amount of catalyst was added to an oven-dried Schlenk tube, followed by addition of CHO and DEC, where applicable. The reaction mixture was degassed and subsequently saturated with CO_2 by repeatedly applying vacuum, followed by addition of 1 bar of CO_2. In experiments monitored by ATR-FTIR spectroscopy, the probe tip was inserted into the reaction mixture via a sealable Schlenk glass adapter. A magnetic stirrer bar was used for mixing. In experiments monitored by ^{1}H NMR spectroscopy, standard Schlenk glassware was employed, and the aliquots were removed at regular time intervals, by opening the Schlenk tube under a countercurrent of CO_2 in order to avoid increased contamination by air or water.

Experiments at CO_2 pressures up to 10 bar were performed in a 100 mL stainless steel Parr reactor equipped with a motorized 4-fold-bladed impeller for stirring. The reaction temperature was regulated by a copper heating mantle block and a thermocouple connected to a Parr 4836 controller unit. The reactor was furthermore equipped with a syringe port valve for aliquot sampling and liquid addition, a gas inlet valve for CO_2 introduction, and an additional valve for applying vacuum or inert gas, as well as a pressure gauge and safety rupture disk. Additionally, the reactor vessel was equipped with a sealable port for introducing the ATR-FTIR probe for in situ measurements. In a typical experiment, a defined amount of catalyst was loaded into the empty reactor, which was then sealed and evacuated. After 5 min, 1 bar of CO_2 was introduced and CHO was added, via the syringe port valve while a slight countercurrent of CO_2 was maintained. After sealing the reactor, the required CO_2 pressure was established, while low-frequency stirring was initiated to support CO_2 dissolution. This step had to be repeated several times until the CO_2 dissolution reached equilibrium and the headspace pressure remained constant. After that, heating was initiated and the stirring rate increased. Aliquots were removed at regular time intervals according to the same method: first, stirring was stopped and the pressure released. An aliquot was taken via the syringe port valve rapidly, before the mixture had time to degas substantially, and the CO_2 pressure was re-established.

Experiments at CO_2 pressures exceeding 10 bar were performed in a customized 2.0 L batch reactor, equipped with a mechanical anchor stirrer with Teflon blades and a maximum stirring rate of 450 rpm. The reactor was heated by an external water-circulating heating mantle reaching temperatures up to 100 °C. Furthermore, the reactor was

equipped with valve ports for CO_2 introduction and liquid addition and a sampling tube with two valves and an internal volume of 10 mL for taking aliquot samples. In a typical experiment, defined amounts of catalyst **1** and CHO were loaded, inside a glovebox, into a pressure-tight metal cylinder, which was subsequently attached to the sealed reactor. By applying CO_2 pressure from the other side of the cylinder, the mixture was forced into the reactor and additional CO_2 was added until the required pressure was obtained; the reactor was then sealed and heating was initiated. Aliquots were taken at regular intervals and analyzed using ^{1}H NMR spectroscopy and GPC, where applicable.

Analysis of Copolymerization Products. ^{1}H NMR spectroscopic analysis of the crude reaction mixture, in $CDCl_3$, was employed to calculate the CHO conversion and reaction selectivity (percent carbonate linkages in PCHC and percent of cyclohexene carbonate byproduct). The composition of the sample was determined by integration of the methylene resonances of poly(cyclohexene carbonate) (PCHC) (4.65 ppm), ether linkages in the copolymer chain (3.45 ppm), cyclic *trans*-cyclohexene carbonate (CHC) (3.9 ppm), and cyclohexene oxide (CHO) (3.07 ppm); the normalized integrals were used to determine the concentrations of the individual components (for an illustrative spectrum, see Supporting Information, Figure S1). The catalyst turnover number (TON) was calculated as the number of moles of CHO converted per mole **1** and the turnover frequency (TOF) as TON per hour, based on the conversions determined by ^{1}H NMR spectroscopy. GPC was used to analyze the samples' number-averaged molecular weights (M_n) and polydispersity indices (PDI), and for these experiments, any contaminating CHO was removed in vacuo and the crude polymer sample was dissolved in THF.

RESULTS AND DISCUSSION

Copolymerization Rate Law. It was essential to determine the copolymerization rate law in order to understand the kinetic parameters and, ultimately, enable the dinuclear mechanistic hypothesis to be tested. Thus, the individual influence of all reagents and the catalyst on the reaction rate was studied by implementing a series of experiments where the only variable was the concentration of the substance of interest. The kinetics experiments to determine the rate law were all conducted at 80 °C, as this was the temperature originally found to give a useful balance between TON and TOF vs low yield of cyclic side product.[11a]

Reaction Order in $[CHO]_0$. The reaction order in cyclohexene oxide (CHO) was determined by two methods. First, four independent experiments were performed with varying CHO concentration (0.825, 1.65, 4.12, and 8.24 M) in diethyl carbonate (DEC). The solvent DEC, necessary for varying the CHO concentration, was chosen because of its structural similarity to the reaction products, the comparably high CO_2 dissolution ability, its chemical inertness under the reaction conditions, and the close similarity of its density compared to CHO.[16] Thus, using DEC, a reaction medium could be established that did not differ significantly from the solvent-free reaction procedure in terms of mass transfer properties and miscibility. The concentration of **1** in all four experiments was 8.3 mM and a total volume of 3 mL was used in a standard Schlenk tube, under a CO_2 pressure of 1 bar. In order to monitor the reaction, aliquots were taken at regular intervals and analyzed by ^{1}H NMR spectroscopy (see Experimental Section). Figure 1 depicts the initial rate (in the linear conversion range between 5 and 20%) of the polymerization reaction vs CHO concentration. The reaction rate undoubtedly showed a linear dependence on the initial CHO concentration, whereby the rate roughly doubled when the initial

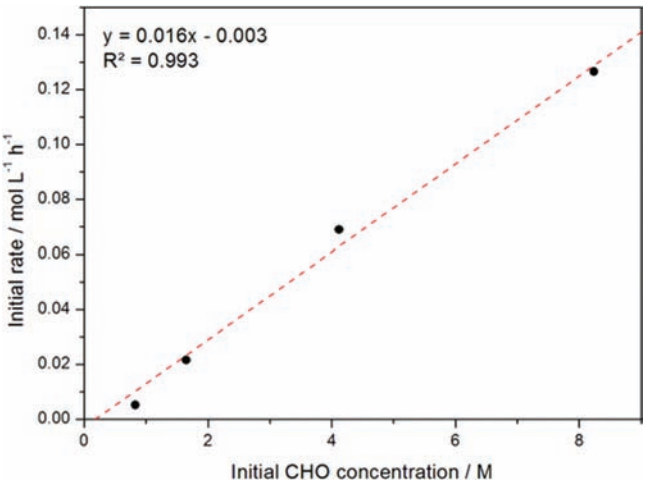

Figure 1. Plot showing the linear fit to the initial rate of copolymerization (M^{-1} h^{-1}) vs the initial concentration of CHO (M). Copolymerization conditions: [**1**] = 8.3 mM, 1 bar of CO_2, in DEC at 80 °C. Initial rates were determined as the slope of fits to plots of $[CHO]_0$ vs time, at $[CHO]_0$ = 0.825, 1.65, 4.12, and 8.24 M, over the range of 5−20% CHO conversion.

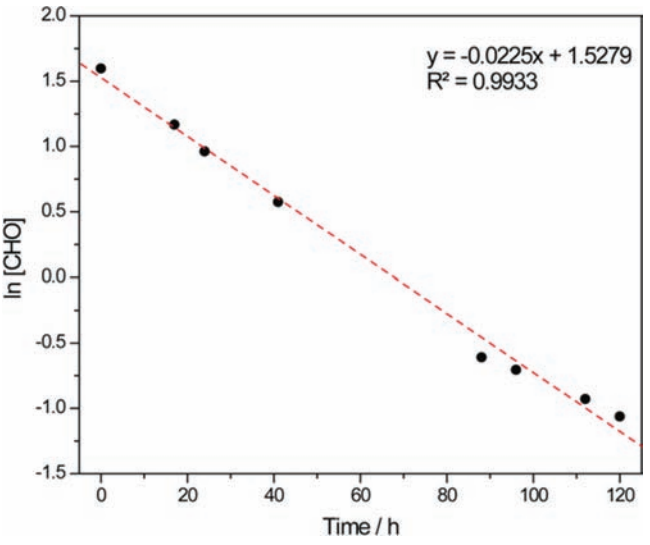

Figure 2. Plot of the ln[CHO] vs time (h) showing a linear fit. Copolymerization conditions: $[CHO]_0$ = 4.94 M, [**1**] = 4.98 mM, in DEC at 80 °C, 1 bar of CO_2, up to 95% conversion (by ^{1}H NMR spectroscopy).

CHO concentration was doubled. This linear dependence strongly suggests a first order of the reaction in [CHO], which leads to the conclusion that despite the dinuclearity of the catalyst only one polymer chain grows per catalyst molecule. In order to further support this finding, the reaction order in [CHO] was also analyzed using an integrated rate law method.[17] Hence, an experiment was performed with 4.94 M CHO, in DEC, and a catalyst concentration of 4.98 mM, at 80 °C and 1 bar CO_2. This reaction was maintained for 120 h until almost full conversion was reached (95% as determined by ^{1}H NMR spectroscopy), in order to exceed several reaction half-lives. A plot of ln[CHO] vs time (Figure 2) clearly exhibited a linear dependence, further corroborating the first-order dependence of

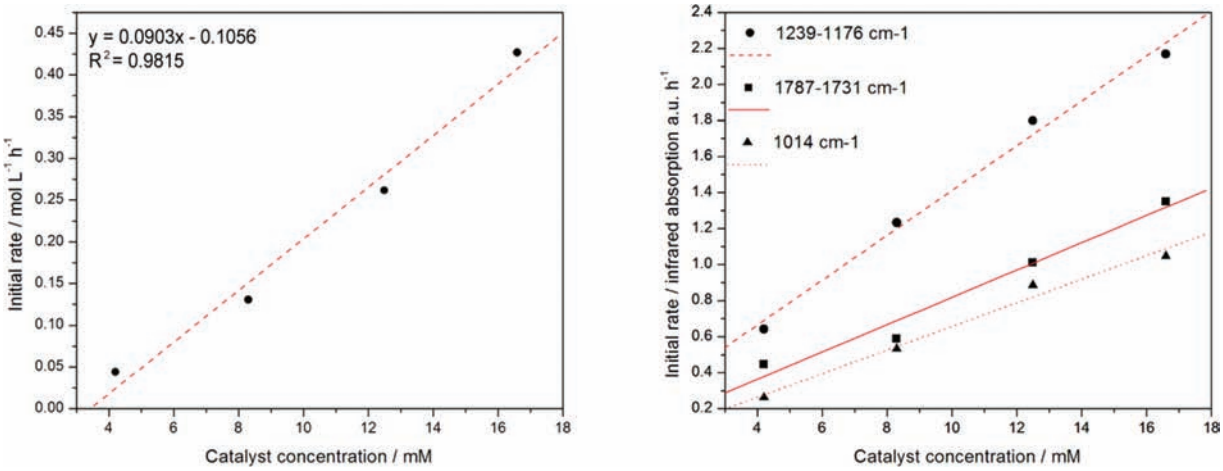

Figure 3. Plots showing the linear fit of the initial rate of polymerization vs the concentration of **1**, as determined by aliquot sampling and subsequent analysis using ^{1}H NMR spectroscopy (left), and the same dependence monitored using in situ ATR-FTIR spectroscopy (right). The ATR-FTIR spectroscopic experiments were monitored using three absorption bands corresponding to molecular vibrations of the polymer. Copolymerization conditions: $[CHO]_0$ = 8.24 M, in DEC at 80 °C and 1 bar of CO_2.

the reaction rate in the concentration of CHO, as determined by the initial rate method. Additionally, the slope of the linear fit corresponds to the rate constant k_{obs}, under these particular conditions, which was used to calculate the reaction half-life, $t_{1/2}$, of 31 h.

Reaction Order in [1]. The reaction order in catalyst concentration was studied over the range [**1**] = 4.2, 8.3, 12.5, and 16.6 mM, with $[CHO]_0$ of 8.24 M in DEC, at 80 °C and 1 bar CO_2. For this study, the results of analysis of aliquots using ^{1}H NMR spectroscopy were verified by repetition of the four experiments using in situ ATR-FTIR spectroscopy. This latter technique is noninvasive, and hence the extent of catalyst deactivation by contaminating air or water during sampling can be minimized, which is especially useful at low catalyst concentrations. It is not possible to directly compare the CHO concentrations in the ATR-IR experiments with those determined using ^{1}H NMR spectroscopy; however, the linear dependence of absorption intensity (using ATR-IR spectroscopy) with CHO concentration still allows for comparative measurements of the reaction rate. The results of both techniques are depicted in Figure 3.

The analysis of aliquots using ^{1}H NMR spectroscopy (Figure 3, left) showed a clear linear relationship between the initial rate and the catalyst concentration, albeit with a slightly less impressive fit to the data. There is a limiting catalyst concentration, manifest by an *x*-axis (catalyst concentration) intercept, corresponding, under these sampling conditions, to [**1**] = 3.42 mM. This arises due to impurities causing catalyst deactivation and inhibiting polymerization; the impurities are likely introduced during sampling for NMR analysis and include excess air and moisture. Closely related effects of impurities resulting in limiting catalyst concentrations have been observed in the analysis of other coordination−insertion polymerization catalysts, for example, using phenolate diamine zinc alkoxide catalysts for lactide polymerization.[18] In a parallel series of experiments, under the same conditions, in situ ATR-FTIR spectroscopy was used to monitor the copolymerization (Figure 3, right). In order to ensure better sensitivity, various vibrational modes were analyzed (details and spectra shown in Supporting Information). These included both the C═O stretching mode (1787−1731 cm^{-1}) of the copolymer, the C−O stretching mode in O−C═O at 1014 cm^{-1}, and the C−O−C asymmetric stretching mode (1239−1176 cm^{-1}); the latter absorption showed approximately twice the gradient (absorption vs time, Figure 3 right) of the other two, probably due to the formation of two C−O−C linkages per repeat unit (compared to the formation of a single C═O linkage per repeat unit). In summary, both methods clearly showed a linear dependence of the initial rate on the catalyst concentration, thereby indicating the reaction was first-order in [**1**]. This contrasts with detailed kinetic studies carried out using zinc β-diiminate catalysts, where the reaction was shown to have a 1.7 order in catalyst concentration, proposed to be due to dimerization occurring to yield the active catalyst.[4c] This interesting mechanistic finding has spurred many other groups into deliberately targeting dinuclear complexes.[10−12,14c,14d] Xiao and coworkers carried out a preliminary mechanistic investigation of a dimagnesium catalysts,[14d] which showed a first-order dependence on catalyst concentration, analogous to that determined in this study. The recent computational study by Lehenmeier et al. using catalyst **1** describes three experiments, in neat CHO and analyzed over the conversion range 0−5%, which were used to suggest an order in catalyst concentration of 1.4; this fractional order was attributed to a "complex reaction network".[15] The orders in monomer concentrations were not determined. Our study does not substantiate these findings, showing a clear linear dependence on catalyst concentration over a wide range of catalyst loadings (from 0.2 to 0.05 mol %).

Reaction Order in [CO_2]. The reaction order in [CO_2] was investigated by varying the initial CO_2 pressure applied to the reactor with an otherwise constant composition of the reaction mixture for each experiment. Due to technical issues, two pressure regimes were investigated using different experiments. First, low-pressure experiments (1−10 bar, initial CO_2 pressure) were monitored by ^{1}H NMR spectroscopic analysis of aliquot samples taken from a 100 mL Parr reactor (see Experimental Section), where the copolymerization was conducted in neat CHO, at CHO:**1** of 8000:1 and at 80 °C. Experiments at higher pressure (10−40 bar, initial CO_2 pressure) were performed in a different reactor system suitable for higher pressure (see

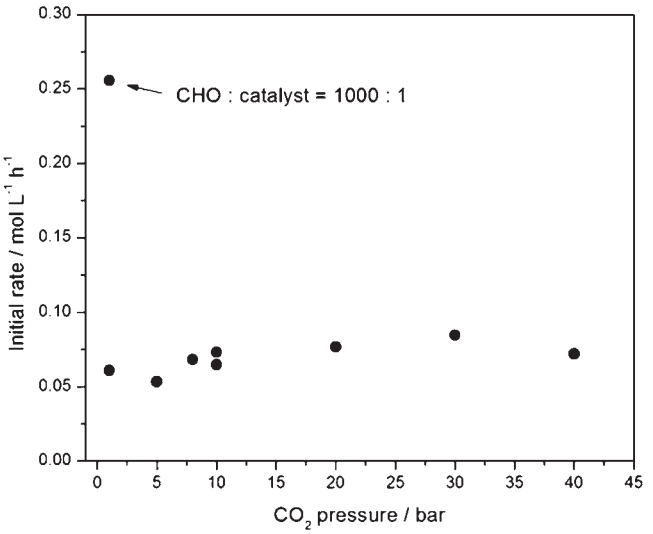

Figure 4. Plot of the initial rate of copolymerization versus the initial CO_2 pressure. The measurements 1−10 bar were using a ratio of CHO:**1** of 8000:1, while the experiments at 10−40 bar were performed in a different reactor and at a ratio of CHO:**1** of 10 000: 1. For comparison, the initial rate obtained at 1 bar of CO_2 pressure, with CHO:**1** of 1000:1 is included. Copolymerization conditions: neat CHO, at 80 °C.

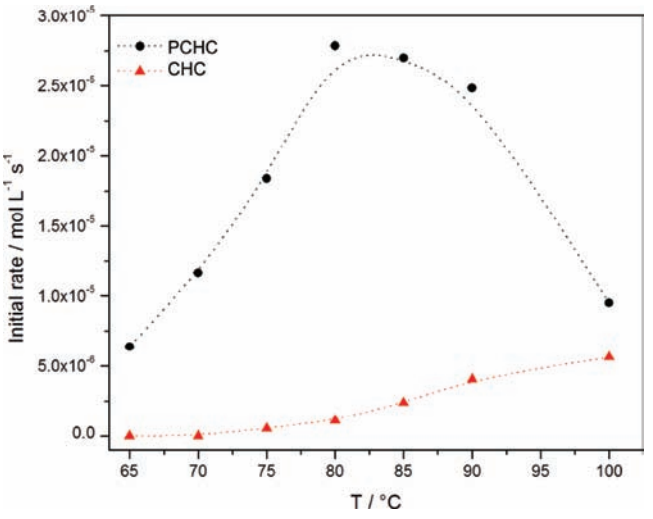

Figure 5. The initial rates of formation of poly(cyclohexene carbonate) (PCHC, circles) and cyclohexene carbonate (CHC, triangles) as a function of the reaction temperature. Copolymerization conditions: $[CHO]_0$ = 4.94 M, [**1**] = 4.98 mM, 1 bar CO_2, in DEC.

Experimental Section). As the reactor volume of the latter system was significantly larger and more CHO had to be used, a higher CHO:**1** ratio of 10 000:1 was employed. The results of this investigation are illustrated in Figure 4. The plot convincingly shows that the initial CO_2 pressure (and thus the CO_2 concentration) had no significant impact on the reaction rate, over the pressure range 1−40 bar. Although the two reactor systems employed for low- and high-pressure experiments make a straightforward comparison somewhat difficult, especially as they do not use exactly the same CHO:catalyst ratio and differ in the reactor volume and stirring mechanism, the resulting relationship between CO_2 pressure and polymerization rate appears to be convincingly independent (within experimental scattering). The initial rate obtained at 1 bar of CO_2 and with a CHO:catalyst ratio of 1000:1 is included for comparison (Figure 4), as it illustrates the much greater impact of catalyst concentration on initial rate compared to CO_2 pressure. Hence, it can be assumed that the reaction rate is virtually independent of CO_2 concentration, at least over the pressure range studied herein. It follows that the rate will be expected to decrease when the CO_2 concentration falls below a critical level, as CO_2 is a monomer in the copolymerization; likewise, it can be expected that the rate will drop at very high CO_2 pressures due to the diluting effect of CO_2-induced swelling of the reaction mixture, as observed elsewhere for related polymer or liquid epoxide systems.[19] In summary, it can be concluded from the independence of the polymer propagation rate on the CO_2 concentration that the reaction is zero order in $[CO_2]$, at least in the pressure range investigated and meaningful for this study.

On the basis of the determination of the reaction order for the reagents and the catalyst, the rate law can be expressed as

$$\text{initial rate} = v_0 = k[\text{CHO}]^1[\text{CO}_2]^0[\mathbf{1}]^1 \quad (1)$$

where the concentrations of the reagents correspond to their initial values and k is the propagation rate constant. The reaction is, thus, first-order in both [CHO] and [**1**], while it is zero-order in $[CO_2]$, over the range of 1 bar $\leq p \leq$ 40 bar.

Activation Energies. The determination of the rate law enables the activation energies for both the copolymerization and the side reactions to be determined. The most significant side reaction is the backbiting reaction to produce cyclic cyclohexene carbonate (CHC). The latter reaction, regarded in this context as unwanted side reaction, must be considered in these copolymerizations, especially those conducted at higher temperatures, as the cyclic carbonate is the thermodynamic product of the reaction between epoxides and CO_2.[4a,8,14c,14d,20] It was of interest to determine the activation energies for PCHC and CHC formation in order to rationalize the catalyst selectivity, under various conditions, and to enable comparisons between this dinuclear catalyst and other reported mononuclear/dimeric systems. The activation energies were determined by monitoring the copolymerization at various temperatures. Experiments were conducted using an initial concentration of CHO of 4.94 M in DEC, a concentration of **1** of 4.98 mM, and a CO_2 pressure of 1 bar. The CO_2 pressure of 1 bar was chosen because of higher accuracy, as Schlenk tubes could be employed with a reduced contamination by impurities, compared to a high-pressure reactor system, and the reaction stirring and heating could be more accurately controlled. The rates of formation for both PCHC and CHC, versus the reaction temperature, are depicted in Figure 5.

It is apparent that there is an optimal temperature for the formation of PCHC (approximately 80 °C), after which the rates of copolymerization decrease with increasing reaction temperature, while the rate of formation of CHC increases with increasing reaction temperature. It was observed that the rates of copolymerization increased exponentially with temperature, up to approximately 80 °C, which is in accordance with the Arrhenius equation.[21] At higher temperatures, a plateau was reached and the rates started to decrease significantly. This effect can be explained by a decrease in the CO_2 solubility, in the liquid phase, with increasing temperature, according to Henry's law.[21] It is apparent that, at temperatures slightly exceeding 80 °C, the solubility of CO_2 (and thus the concentration in solution)

dx.doi.org/10.1021/ja206352x |J. Am. Chem. Soc. 2011, 133, 17395–17405

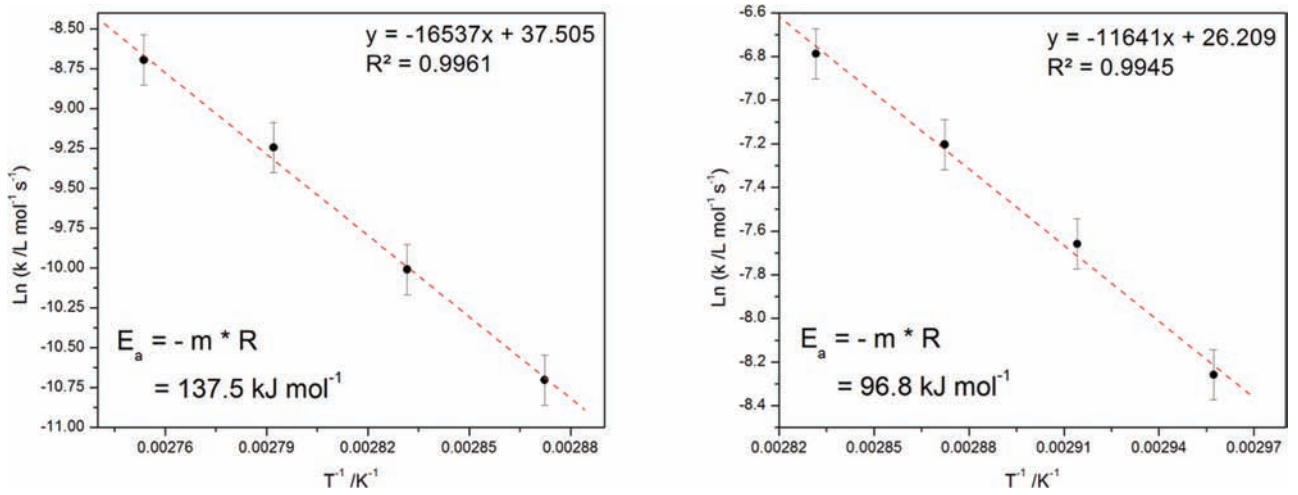

Figure 6. Arrhenius plots for the formation of poly(cyclohexene carbonate) (PCHC, left) and cyclohexene carbonate (CHC, right). The equations for the linear fit are given in the top right corners, while the activation energies are given in the bottom left corners as insets. Copolymerization conditions: $[CHO]_0$ = 4.94 M, [**1**] = 4.98 mM, in DEC at 1 bar of CO_2.

at 1 bar of pressure reaches a critically low value and becomes a limiting factor in the reaction. Thus, the rate law with zero order in $[CO_2]$ is no longer valid once the reaction temperature exceeds 80 °C. Therefore, the determination of the activation energies for the formation of PCHC used four data points between 60 and 80 °C (vide infra). For CHC, the temperature effect of CO_2 solubility is not as significant, and a plateau or a decrease in reaction rate was not observable with increasing temperature. The reason for this is that the rate of formation of CHC is not directly dependent on $[CO_2]$, as CHC is only formed from catalyst-bound PCHC as a subsequent product, and as long as there are sufficient catalyst-bound polymer chains present, the rate of CHC formation will not be affected by depleting CO_2. Nevertheless, as shown if Figure 5, when the rates for PCHC start to decrease most rapidly, the rates for CHC also start to decrease, observable by the slight dampening of the exponential increase in the rates with temperature. In order to minimize this effect when calculating the activation energy, only four data points were used for the calculation over the temperature range 70−85 °C. For both products, the rates at the corresponding temperatures were used to calculate the corresponding propagation rate constants *k*, which were used to determine the activation energies via Arrhenius plots. The Arrhenius plots for both PCHC and CHC are depicted in Figure 6.

The experimentally determined activation energies for the formation of PCHC and CHC are 96.8 ± 1.6 and 137.5 ± 6.4 kJ mol^{-1}, respectively. A schematic energetic reaction pathway for the two products is shown is Figure 7.

The activation energies (E_a) are somewhat higher than equivalent values determined for other CHO/CO_2 copolymerization catalysts, especially for PCHC. For example, Darensbourg et al. determined activation energies of just 46.9 kJ mol^{-1} for PCHC and 133.0 kJ mol^{-1} for CHC, using a chromium−salen based catalyst.[8] While the E_a for CHC is in a comparable range, the value for PCHC is almost twice this value using catalyst **1**. Similarly, Xiao et al. recently investigated the reaction kinetics for CHO/CO_2 copolymerization catalyzed by a dinuclear magnesium catalyst.[14d] They found activation energies of 45.3 kJ mol^{-1} for PCHC and 127.2 kJ mol^{-1} for CHC, values within the same range as those determined by Darensbourg. The comparably

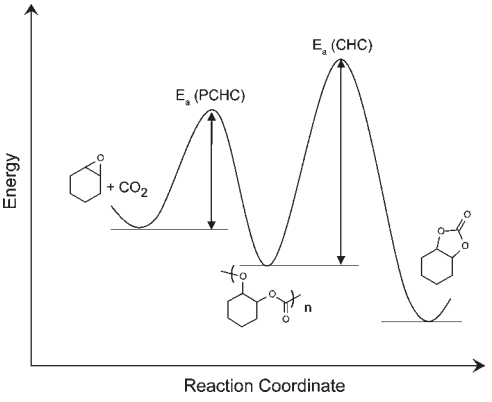

Figure 7. Schematic energetic reaction pathway for the formation of both possible products poly(cyclohexene carbonate) (PCHC) and cyclohexene carbonate (CHC) with experimentally determined E_a(PCHC) of 96.8 kJ mol^{-1} and E_a(CHC) of 137.5 kJ mol^{-1}.

high activation energy for the formation of PCHC catalyzed by **1** explains the relatively high temperatures (>60 °C) required for this process, despite the advantage of it operating at ambient CO_2 pressure. On the other hand, the energetic difference between PCHC and CHC is still sufficiently high to maintain an excellent selectivity toward PCHC when using **1** as catalyst. Although this somewhat higher activation energy for PCHC can be regarded a disadvantage, catalyst **1** is, on the other hand, still producing polymer with excellent control compared to other ambient pressure systems.[14c,d,22]

Proposed Mechanism. On the basis of the results of the kinetics investigation, a detailed mechanism can be proposed, which is depicted in Scheme 2.

The initiation step consists of a nucleophilic attack of the initiating group (in this case acetate) on a molecule of CHO, which has been activated by coordination at one of the zinc centers. This initiation step is rather slow, reflected by the initiation time (usually 30 min) required for the reaction to start, as observed by in situ ATR-IR spectroscopy. Initiation leads to formation of a propagating zinc alkoxide species, which is regarded as one of the active catalyst species. The subsequent

Scheme 2. Proposed Mechanism of the Copolymerization of CO_2 and Cyclohexene Oxide (CHO) Catalyzed by 1[a]

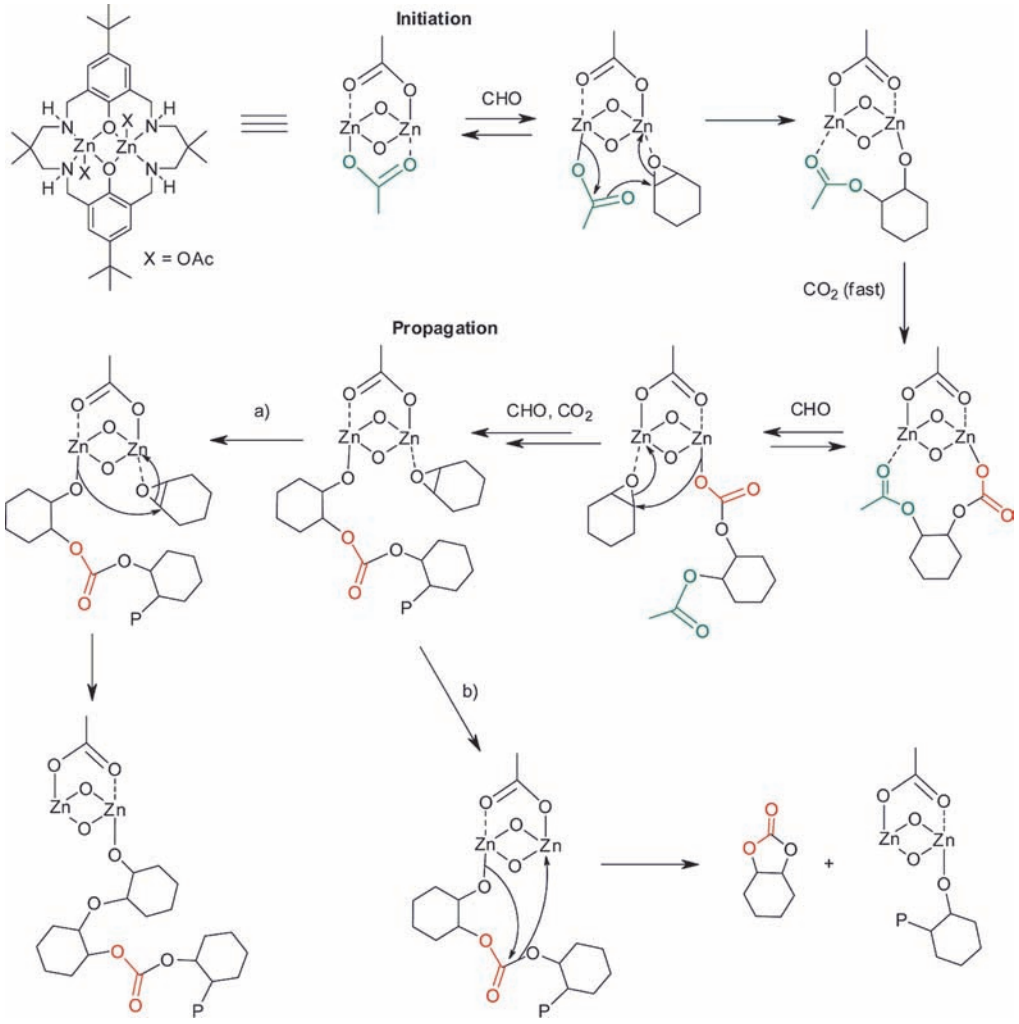

[a] Possible side reactions include (a) ether linkage formation and (b) cyclic carbonate formation. The macrocyclic ligand is omitted for clarity in the mechanistic pathway.

insertion of CO_2 into the zinc−alkoxide bond must proceed very rapidly, supported by the zero reaction order in CO_2. The second bridging acetate group, located on the other side of the macrocyclic ligand plane, is not proposed to be active as a propagating site (as the first-order reaction in **1** and CHO accordingly suggests) but rather ensures both Zn centers can maintain an octahedral coordination sphere and neutral charge balance throughout the whole reaction. One reason for this might be that the axial positions of the macrocyclic ligand have different steric accessibilities under the reaction conditions. The propagation cycle continues with nucleophilic attack of the carbonate species on a coordinated CHO molecule to generate a new zinc−alkoxide bond, into which CO_2 can rapidly insert, and so on. The chain probably changes the zinc center at which it is coordinated with every repeat unit (sequence of ring-opening and CO_2 insertion), which would explain the high activity of such dinuclear complexes, as well as rationalizing how coordination and charge balance at the zinc centers are maintained. Scheme 2 also illustrates two possible side reactions, the attack of the putative zinc alkoxide intermediate on a second molecule of CHO leading to ether linkages (pathway a) and the formation of cyclic cyclohexene carbonate (CHC; pathway b). The formation of ether linkages scarcely occurs using **1**; the proportion of ether linkages is usually between 2 and 5% or less, as determined by ^{1}H NMR spectroscopy. The formation of ether linkages can be undesirable, as it decreases thermal and mechanical stability of the resulting copolymers; the rationale for the low degree of ether formation using **1** probably results from the reduction in the Lewis acidity (mediation of electronic properties) of the zinc centers conferred by the electron-donating macrocyclic ancillary ligand. This hypothesis is supported by a copolymerization experiment, using $Zn(OAc)_2$ as the catalyst (Table 1, entry 4). The overall activity of $Zn(OAc)_2$ was much lower than **1** (Table 1, entry 4), with as much as 40% of the product consisting of ether linkages. The macrocyclic ancillary ligand in **1** thus not only increases the activity but also suppresses the undesired ether linkage formation. The latter side reaction, the formation of CHC, occurs via backbiting of the growing polymer chain in a depolymerisation process. This step is mainly temperature-dependent (vide supra), as CHC is thermodynamically more stable, but requires significantly higher activation energy. While working at 1 bar of CO_2, the formation of CHC can be almost

dx.doi.org/10.1021/ja206352x |*J. Am. Chem. Soc.* 2011, 133, 17395–17405

Table 1. Copolymerization of CHO and CO_2 Using 1, with Various Species Added as Chain Transfer Agents (CTA). [a]

entry	catalyst (mol %)	TON[b]	TOF[c] (h^{-1})	CHO conversion (%)	$S_{carbonates}$[d] (%)	S_{PCHC}[e] (%)	M_n[f] (g mol^{-1})	PDI (M_w/M_n)[f]
1	0.1% **1**	530	22	53	99	92	10949	1.02
							5022	1.02
2	0.1% **1** + 0.1% CHD[g]	580	24	58	99	93	8516	1.04
							3588	1.09
							(1025)	(1.18)
3	0.1% **1** + 2% H_2O	610	25	61	99	93	3428	1.06
							1280	1.01
4	0.2% $Zn(OAc)_2$	175[h]	7[h]	35	60	94	–[i]	–[i]

[a] Copolymerization conditions: neat CHO, 80 °C, 24 h, 1 bar of CO_2. [b] TON = $mol_{CHO\ converted} \times (mol_1)^{-1}$. [c] TOF = TON per hour. [d] $S_{carbonate}$ = Percentage selectivity for carbonate linkages (PCHC + CHC), as determined from the normalized integrals in the ^1H NMR spectra using the methylene resonances, including PCHC (δ 4.65 ppm), ether linkages (δ 3.45 ppm), and CHC (δ 3.9 ppm). [e] Selectivity for PCHC within carbonate products. [f] Determined by GPC, in THF, using narrow M_n polystyrene standards, for calibration. [g] CHD = cyclohexane-1,2-diol. [h] Calculated on the basis of $mol_{CHO\ converted} \times (mol_{Zn})^{-1}$. [i] Could not be determined satisfactorily. GPC trace showed an extremely broad distribution of polymer chains of random M_n.

completely suppressed, if the temperature is kept at or below 80 °C. Higher temperatures would anyway require higher pressures for sufficient CO_2 solubility (vide supra), while lower temperatures decrease the reaction rate too severely due to the relatively high activation energy.

PCHC Characterization. It has frequently been observed that PCHC, as well as other copolymers formed by epoxide/CO_2 coupling, display a bimodal distribution of number-averaged molecular weights, regardless of the catalysts employed.[7h,i,12−14,23] Two key features of this bimodality are that both distributions normally have a very narrow polydispersity index (PDI), while the higher molecular weight distribution frequently exhibits approximately twice the M_n of the lower molecular weight distribution. Aida and Inoue first discovered this effect in the copolymerization of phthalic anhydride and propylene oxide, catalyzed by an aluminum porphyrin/quarternary salt system.[23b] They attributed it to mechanisms where polymer chains could grow from both sides of the ligand plane, which led to two competing mechanisms (single chain growth versus double chain growth) with different catalytic activity. The same explanation was proposed by Sugimoto et al. for the copolymerization of CHO and CO_2, catalyzed by an aluminum Schiff base/ammonium salt system.[23a] This explanation, however, is less convincing for catalyst **1**, because the ligand lacks the rigid planarity usually required for a chain growth on both faces of the molecule. Furthermore, the rate law clearly shows a first-order dependence in catalyst and monomer concentrations, ruling out growth of two chains per catalyst (which would be expected to show a second-order dependence in monomer concentration, or at least not clearly a first-order dependence). In order to investigate the bimodal molecular weight distribution more thoroughly, PCHC samples displaying distinctly bimodal distributions, by GPC, were analyzed by MALDI-ToF spectrometry. This technique enables the determination of the PCHC end groups, at least for those chains that are volatilized. A typical MALDI-ToF spectrum, the corresponding GPC trace, and an assignment of the end groups, is illustrated in Figure 8.

The MALDI-ToF spectra showed a bimodal molecular weight distribution, with the higher M_n series corresponding to PCHC chains end-capped with a hydroxyl group and a cyclohexan-2-ol group while the lower M_n series were end-capped with an acetate and a cyclohexan-2-ol group, as expected from the initiation mechanism. The finding that the longer chains were terminated with hydroxyl groups at both chain ends was initially surprising and led us to consider whether coupling reactions, chain degradation, or similar phenomena could be occurring, as were proposed by Duchateau et al. using silesquioxane-based alkyl zinc catalysts.[24] Such mechanisms are unlikely for catalyst **1**, because they would not be expected to reproducibly yield bimodal distributions of molecular weights, especially with a consistent chain length ratio of 2:1 and narrow PDIs. Interestingly, the same bimodal distributions, with the longer chains end-capped with hydroxyl groups and the shorter chains end-capped with hydroxyl and initiating groups, were observed for polycarbonates prepared using a range of other catalysts. Examples include reports by Nakano et al., using chromium complexes coordinated by partially reduced salen ligands;[7i] Sugimoto et al., using aluminum salen catalysts;[23a] and by our group, using iron[13] and cobalt[12] complexes of the same ligand as **1**. For complex **1**, mechanisms involving the propagation of two polymer chains per catalyst (including a coupling at the end of the reaction or a remaining incorporated catalyst molecule) would contradict the first-order reaction in **1**. Also, any postreaction mechanism (such as hydrolysis, decarboxlation, or other degradation) as described elsewhere[24,25] would not explain the narrow PDI, as such degradation processes would occur randomly and lead to much broader PDIs than observed. Therefore, an alternative explanation and mechanism is proposed to rationalize the bimodality, as illustrated in Scheme 3.

It is proposed that at/near the start of reaction, cyclohexane-1,2-diol, produced by the hydrolysis of CHO and present in trace quantities, acts as a chain transfer agent (CTA) (step a). It is already established that rapid and reversible chain transfer reactions with alcohols and/or water readily occur in epoxide/CO_2 copolymerization using a wide range of catalyst systems.[7i,14a,23a,26] The chain transfer reactions are fast and reversible, and occur significantly faster than propagation, leading to narrow molecular weight distributions and to immortal polymerization.[27] In an immortal polymerization it is proposed that all chains propagate at the same/very similar rate and that the number of chains is determined by the concentration of catalyst + CTA; this contrasts with controlled/living polymerizations, where it is only the concentration of catalyst that determines the number of chains. Assuming immortal polymerization occurs, cyclohexane-1,2-diol undergoes chain transfer reactions, leading to a new initiating species (a diol) that can propagate from both of the two hydroxyl end groups (Scheme 3, step b). The chains initiated from

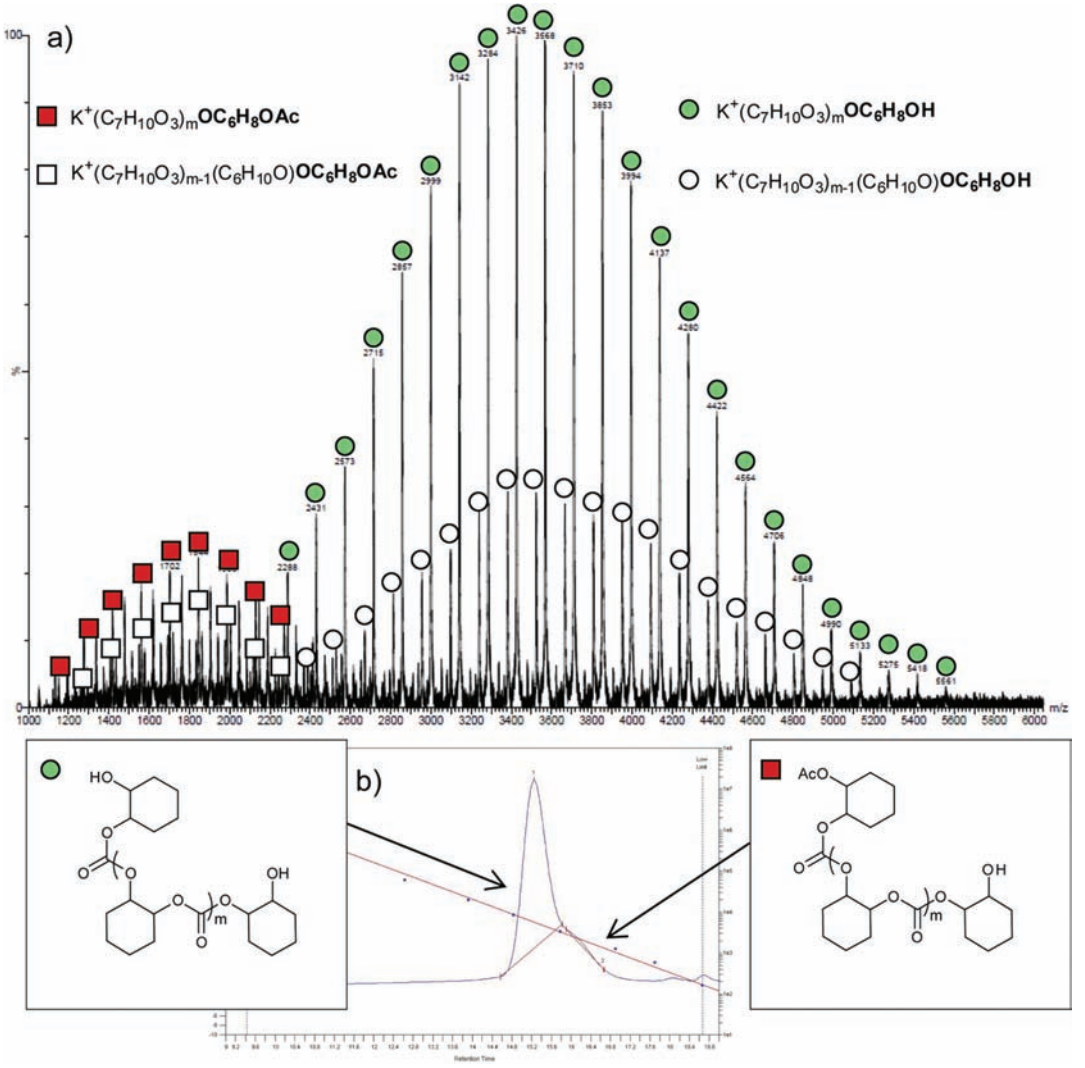

Figure 8. (a) Typical MALDI-ToF spectrum including the formulas used for the assignment of the mass fractions (inset) and (b) corresponding GPC trace of a polymer with a bimodal chain length distribution. The main distribution with higher molecular mass consisted of chains end-capped with hydroxyl groups (filled circles), and the lower mass distribution was assigned to have acetate end groups (filled squares). Each distribution had a secondary distribution with one ether linkage (open symbols). The PCHC was obtained after 20 h reaction time at 80 °C and 20 bar of CO_2 pressure in neat CHO with CHO:**1** = 8000:1.

cyclohexane-1,2-diol can thus grow from both chain ends, while those initiated from acetate groups can only grow from a single chain end. Hence, the chains initiated from cyclohexane-1,2-diol will grow by two repeat units per propagation cycle, while the chains initiated from acetate will only grow by a single repeat unit per propagation cycle. As long as the conditions of immortal polymerization are met, the chains initiated from cyclohexane-1,2-diol will be expected to have approximately double the chain lengths (and thus M_n) compared to the chains initiated from acetate, regardless of reaction time, and the polydispersity indices of both chain types are expected to be narrow. As both hydroxyl−hydroxyl and acetate−hydroxyl chain end groups are observed, the concentration of cyclohexane-1,2-diol present must be lower than the concentration of dizinc acetate. In order to support this assumption further, and to investigate whether cyclohexane-1,2-diol or water (or both) is responsible, experiments were performed where cyclohexane-1,2-diol (CHD) or water was added at the start of the reaction. The results are summarized in Table 1.

Entry 1 shows a standard experiment using purified and dried CHO for comparison. Despite the purification of the CHO, which included drying over CaH_2 and fractional distillation, the PCHC exhibited a clear bimodal distribution of molecular weight, with a relative ratio of M_n values of 2:1. Although the ^{1}H NMR spectra of freshly distilled CHO did not show any impurities, it is still quite possible that a concentration of diol or water below the detection limit of ^{1}H NMR contributed to this effect. An experiment was performed under identical conditions (Table 1, entry 2), but addition of an equimolar amount (vs **1**) of CHD to the system corroborated this assumption. The overall catalytic activity and the product selectivity were not hampered; however, the M_n was reduced, and two slightly overlapping yet discrete M_n distributions of narrow PDI were obtained. Additionally, a broad distribution of short oligomers of around 1000 g mol^{-1} was observed, which however was very close to lower calibration limit of the GPC instrument. It appears that diols, such as CHD, have an impact on the PCHC M_n and

Scheme 3. Proposed Mechanism To Rationalize the Bimodal Molecular Weight Distributions[a]

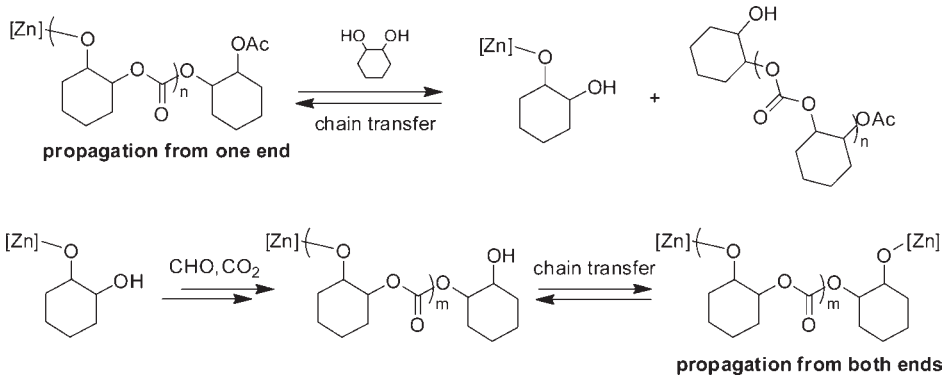

[a] Two processes are proposed to occur: (a) early chain transfer reactions with cyclohexenediol leads to the formation of hydroxyl-terminated polymer chains and (b) hydroxyl-terminated chains are able to grow from both ends, via fast chain transfer reactions, to yield telechelic PCHC. The dizinc complex **1** is denoted as [Zn] for clarity.

distribution, but they do not interfere with the catalytic activity. This implies that CHD is a chain transfer agent, leading to PCHC end-capped with two hydroxyl groups. The hydroxyl end groups were confirmed by MALDI-ToF analysis. The MALDI-ToF spectrum of the dried polymer of this experiment is included in the Supporting Information (Figure S10). The source of the CHD in the standard reactions is difficult to elucidate; it is possible that traces contaminate the distilled CHO, perhaps due to strong interactions (such as hydrogen bonding), or it could be that the hydrolysis of CHO, by trace quantities of water, leads to formation of CHD in situ. This would likely be accelerated at the elevated temperature during copolymerization. Sources of water could include insufficiently dried CO_2, glassware, and other equipment, and, of course, the CHO itself. In order to investigate this, an experiment was performed where water was deliberately added to the system (a 20-fold excess compared to **1**; Table 1, entry 3). Once again, the activity, in terms of TOF and conversion, remained unchanged, or even slightly increased. This may be due to the production of lower M_n PCHC, which had lower viscosity compared to the benchmark experiment (Table 1, entry 1). The observation that the catalytic activity was not decreased upon addition of even a 20-fold excess of water strongly implies that the hydrolysis of CHO occurs readily. The putative propagating Zn alkoxides are expected to be highly sensitive toward hydrolysis, and such a reaction would form zinc hydroxide species. We cannot discount the possibility that zinc hydroxide groups could initiate copolymerization; however, all attempts to synthesize a derivate of **1** with hydroxide coligands have failed, most probably due to the sensitivity of such species to further decomposition reactions. Known zinc hydroxide-based catalysts, such as the early $ZnEt_2-H_2O$ catalyst reported by Inoue et al. and subsequent heterogeneous catalyst derivatives, could not be completely structurally clarified, and the polymers produced from such systems were much less uniform in terms of chain length.[2] Also, a hydroxyl-substituted zinc β-diiminate complex reported by Coates et al. showed no catalytic activity in the copolymerization of CO_2 and epoxides.[6b] Therefore, it seems likely that the addition of water to the reaction does not impede the catalysis but rather leads to chain transfer, most likely due to in situ hydrolysis of CHO. The PCHC produced in this experiment showed a low M_n, with the expected bimodal distribution and narrow PDI. It is interesting to note the tolerance of catalyst **1**, even with excess contaminating water. This is in contrast to aluminum porphyrin-catalyzed copolymerization of CO_2 and propylene oxide recently reported by Chatterjee and Chisholm, where the authors found evidence that their observed bimodality was caused by adventitious water contamination as well.[23c] However, they attributed it to partial hydrolysis of their catalyst and formation of a new, less active catalytic species, which yielded the lower mass fraction of the bimodal polymer. A related explanation for the bimodality observed using complex **1** seems unlikely, for the reasons outlined above regarding zinc hydroxide activity and control.

■ CONCLUSIONS

The kinetics of the copolymerization of CO_2 and CHO, catalyzed by the dizinc complex **1**, was investigated using in situ ATR-FTIR and ^{1}H NMR spectroscopy. The parameter studies revealed a zero-order dependence on $[CO_2]$, for the pressure range 1 bar $\leq p \leq$ 40 bar, and a first-order dependence for both the initial [CHO] and [**1**]. This finding strongly supports the hypothesis that CO_2 insertion is not the rate-determining step, at least under these conditions, and only becomes limiting at temperatures exceeding 80 °C. The reaction temperature screening, using 1 bar of CO_2 pressure, provided insights into the boundary conditions for CO_2 solubility at higher temperatures and allowed calculation of the activation energies for the formation of PCHC and cyclic CHC. Catalyst **1** was found to operate optimally at 80 °C and 1 bar of CO_2, reaching a TOF of 15 h^{-1} in neat CHO and producing PCHC with 99% selectivity for carbonate linkages and 96% selectivity for PCHC. The PCHC produced was analyzed by GPC and MALDI-ToF spectrometry, which revealed two narrow number-average molecular weight distributions, exhibiting an almost constant ratio of molecular weights (chain lengths). It was consistently observed that the higher molecular weight distribution was approximately double the mass of the lower molecular weight distribution. The higher M_n series were assigned, by MALDI-ToF, to PCHC end-capped by hydroxyl groups, while the lower M_n distribution was due to PCHC end-capped with acetate and hydroxyl groups. Additional experiments were conducted where various equivalents of cyclohexane-1,2-diol and water were added; this, with the characterization data, led to a proposal that rapid and reversible chain transfer reactions can occur and that, under certain

conditions, the polymerizations are immortal. The catalyst was remarkably robust, in terms of its tolerance to excess quantities of water or cyclohexane-1,2-diol, yet the PCHC molecular weight is strongly influenced by such impurities.

■ ASSOCIATED CONTENT

Supporting Information. Characterization of polymers by NMR and MALDI-TOF, complete kinetic data (NMR and ATR-FTIR), including all the fits and tabulated data, and complete ref 1a. This material is available free of charge via the Internet at http://pubs.acs.org.

■ AUTHOR INFORMATION

Corresponding Author
c.k.williams@imperial.ac.uk

■ ACKNOWLEDGMENT

Norner AS (Stathelle, Norway), the Leverhulme foundation (F/07 058/BD), the EPSRC (EP/C544846/1 and EP/C544838/1) are acknowledged for funding this research.

■ REFERENCES

(1) (a) Arakawa, H.; et al. *Chem. Rev.* **2001**, *101*, 953. (b) Aresta, M.; Dibenedetto, A. *Dalton Trans.* **2007**, 2975. (c) Behr, A. *Angew. Chem., Int. Ed.* **1988**, *27*, 661. (d) Jessop, P. G.; Ikariya, T.; Noyori, R. *Chem. Rev.* **1995**, *95*, 259. (e) Leitner, W. *Coord. Chem. Rev.* **1996**, *153*, 257. (f) MacDowell, N.; Florin, N.; Buchard, A.; Hallett, J.; Galindo, A.; Jackson, G.; Adjiman, C. S.; Williams, C. K.; Shah, N.; Fennell, P. *Energy Environ. Sci.* **2010**, *3*, 1645.

(2) Inoue, S.; Koinuma, H.; Tsuruta, T. *J. Polym. Sci., Part B: Polym. Lett.* **1969**, *7*, 287.

(3) (a) Klaus, S.; Lehenmeier, M. W.; Anderson, C. E.; Rieger, B. *Coord. Chem. Rev.* **2011**, *255*, 1460. (b) Coates, G. W.; Moore, D. R. *Angew. Chem., Int. Ed.* **2004**, *43*, 6618. (c) Darensbourg, D. J. *Chem. Rev.* **2007**, *107*, 2388. (d) Nozaki, K.; Nakano, K.; Hiyama, T. *J. Am. Chem. Soc.* **1999**, *121*, 11008. (e) Sugimoto, H.; Inoue, S. *J. Polym. Sci., Part A: Polym. Chem.* **2004**, *42*, 5561. (f) Kember, M. R.; Buchard, A.; Williams, C. K. *Chem. Commun.* **2011**, *47*, 141.

(4) (a) Darensbourg, D. J.; Yarbrough, J. C. *J. Am. Chem. Soc.* **2002**, *124*, 6335. (b) Mang, S.; Cooper, A. I.; Colclough, M. E.; Chauhan, N.; Holmes, A. B. *Macromolecules* **1999**, *33*, 303. (c) Moore, D. R.; Cheng, M.; Lobkovsky, E. B.; Coates, G. W. *J. Am. Chem. Soc.* **2003**, *125*, 11911. (d) Moore, D. R.; Cheng, M.; Lobkovsky, E. B.; Coates, G. W. *Angew. Chem., Int. Ed.* **2002**, *41*, 2599. (e) Bok, T.; Yun, H.; Lee, B. Y. *Inorg. Chem.* **2006**, *45*, 4228.

(5) Koning, C.; Wildeson, J.; Parton, R.; Plum, B.; Steeman, P.; Darensbourg, D. J. *Polymer* **2001**, *42*, 3995.

(6) (a) Cheng, M.; Lobkovsky, E. B.; Coates, G. W. *J. Am. Chem. Soc.* **1998**, *120*, 11018. (b) Cheng, M.; Moore, D. R.; Reczek, J. J.; Chamberlain, B. M.; Lobkovsky, E. B.; Coates, G. W. *J. Am. Chem. Soc.* **2001**, *123*, 8738. (c) Eberhardt, R.; Allmendinger, M.; Luinstra, G. A.; Rieger, B. *Organometallics* **2003**, *22*, 211. (d) Allen, S. D.; Moore, D. R.; Lobkovsky, E. B.; Coates, G. W. *J. Am. Chem. Soc.* **2002**, *124*, 14284.

(7) (a) Darensbourg, D. J.; Mackiewicz, R. M. *J. Am. Chem. Soc.* **2005**, *127*, 14026. (b) Cohen, C. T.; Chu, T.; Coates, G. W. *J. Am. Chem. Soc.* **2005**, *127*, 10869. (c) Qin, Z.; Thomas, C. M.; Lee, S.; Coates, G. W. *Angew. Chem., Int. Ed.* **2003**, *42*, 5484. (d) Shi, L.; Lu, X.-B.; Zhang, R.; Peng, X.-J.; Zhang, C.-Q.; Li, J.-F.; Peng, X.-M. *Macromolecules* **2006**, *39*, 5679. (e) Noh, E. K.; Na, S. J.; Sujith, S.; Kim, S. W.; Lee, B. Y. *J. Am. Chem. Soc.* **2007**, *129*, 8082. (f) Sujith, S.; Min, J. K.; Seong, J. E.; Na, S. J.; Lee, B. Y. *Angew. Chem., Int. Ed.* **2008**, *47*, 7306. (g) Luinstra, G. A.; Haas, G. R.; Molnar, F.; Bernhart, V.; Eberhardt, R.; Rieger, B. *Chem.—Eur. J.* **2005**, *11*, 6298. (h) Nakano, K.; Kamada, T.; Nozaki, K. *Angew. Chem., Int. Ed.* **2006**, *45*, 7274. (i) Nakano, K.; Nakamura, M.; Nozaki, K. *Macromolecules* **2009**, *42*, 6972.

(8) Darensbourg, D. J.; Yarbrough, J. C.; Ortiz, C.; Fang, C. C. *J. Am. Chem. Soc.* **2003**, *125*, 7586.

(9) (a) Vagin, S. I.; Reichardt, R.; Klaus, S.; Rieger, B. *J. Am. Chem. Soc.* **2010**, *132*, 14367. (b) Nakano, K.; Hashimoto, S.; Nozaki, K. *Chem. Sci.* **2010**, *1*, 369.

(10) Lee, B. Y.; Kwon, H. Y.; Lee, S. Y.; Na, S. J.; Han, S.-i.; Yun, H.; Lee, H.; Park, Y.-W. *J. Am. Chem. Soc.* **2005**, *127*, 3031.

(11) (a) Kember, M. R.; Knight, P. D.; Reung, P. T. R.; Williams, C. K. *Angew. Chem., Int. Ed.* **2009**, *48*, 931. (b) Kember, M. R.; White, A. J. P.; Williams, C. K. *Inorg. Chem.* **2009**, *48*, 9535.

(12) Kember, M. R.; White, A. J. P.; Williams, C. K. *Macromolecules* **2010**, *43*, 2291.

(13) Buchard, A.; Kember, M. R.; Sandeman, K. G.; Williams, C. K. *Chem. Commun.* **2011**, *47*, 212.

(14) (a) Sugimoto, H.; Kuroda, K. *Macromolecules* **2008**, *41*, 312. (b) Sugimoto, H.; Ohtsuka, H.; Inoue, S. *J. Polym. Sci., Part A: Polym. Chem.* **2006**, *43*, 4172. (c) Xiao, Y. L.; Wang, Z.; Ding, K. L. *Chem.—Eur. J.* **2005**, *11*, 3668. (d) Xiao, Y. L.; Wang, Z.; Ding, K. L. *Macromolecules* **2006**, *39*, 128.

(15) Lehenmeier, M. W.; Bruckmeier, C.; Klaus, S.; Dengler, J. E.; Deglmann, P.; Ott, A.-K.; Rieger, B. *Chem. Eur. J.* **2011**, *17*, 8858–8869.

(16) Blanchard, F.; Carre, B.; Bonhomme, F.; Biensan, P.; Lemordant, D. *Can. J. Chem.* **2003**, *81*, 385.

(17) Pilling, M. J.; Seakins, P. W. *Reaction Kinetics*; Oxford University Press: Oxford, 1997.

(18) Williams, C. K.; Breyfogle, L. E.; Choi, S. K.; Nam, W.; Young, V. G.; Hillmyer, M. A.; Tolman, W. B. *J. Am. Chem. Soc.* **2003**, *125*, 11350.

(19) (a) Guadagno, T.; Kazarian, S. G. *J. Phys. Chem. B* **2004**, *108*, 13995. (b) Jutz, F.; Grunwaldt, J. D.; Baiker, A. *J. Mol. Catal. A: Chem.* **2008**, *279*, 94.

(20) (a) Darensbourg, D. J.; Moncada, A. I.; Choi, W.; Reibenspies, J. H. *J. Am. Chem. Soc.* **2008**, *130*, 6523. (b) Darensbourg, D. J.; Niezgoda, S. A.; Draper, J. D.; Reibenspies, J. H. *J. Am. Chem. Soc.* **1998**, *120*, 4690.

(21) Gold, V.; Loening, K. L.; McNaught, A. D. *IUPAC Compendium of Chemical Terminology*; International Union of Pure and Applied Chemistry: Research Triangle Park, NC, 1991.

(22) (a) Sugimoto, H.; Ohshima, H.; Inoue, S. *J. Polym. Sci., Part A: Polym. Chem.* **2003**, *41*, 3549. (b) Vitanova, D. V.; Hampel, F.; Hultzsch, K. C. *J. Organomet. Chem.* **2005**, *690*, 5182.

(23) (a) Sugimoto, H.; Ohtsuka, H.; Inoue, S. *J. Polym. Sci., Part A: Polym. Chem.* **2005**, *43*, 4172. (b) Aida, T.; Inoue, S. *J. Am. Chem. Soc.* **1985**, *107*, 1358. (c) Chatterjee, C.; Chisholm, M. H. *Inorg. Chem.* **2011**, *50*, 4481.

(24) Duchateau, R.; van Meerendonkt, W. J.; Huijser, S.; Staal, B. B. P.; van Schilt, M. A.; Gerritsen, G.; Meetsma, A.; Koning, C. E.; Kemmere, M. F.; Keurentjes, J. T. F. *Organometallics* **2007**, *26*, 4204.

(25) Liu, B.; Chen, L.; Zhang, M.; Yu, A. *Macromol. Rapid Commun.* **2002**, *23*, 881.

(26) (a) van Meerendonk, W. J.; Duchateau, R.; Koning, C. E.; Gruter, G. J. M. *Macromolecules* **2005**, *38*, 7306. (b) Cyriac, A.; Lee, S. H.; Lee, B. Y. *Polym. Chem.* **2011**, *2*, 950.

(27) (a) Inoue, S. *J. Polym. Sci., Part A: Polym. Chem.* **2000**, *38*, 2861. (b) Iván, B. *Macromol. Symp.* **1994**, *88*, 201.